PCCP

ROYAL SOCIETY OF CHEMISTRY

PAPER

View Article Online
View Journal | View Issue

Cite this: *Phys. Chem. Chem. Phys.*, 2025, **27**, 5080

Carotenoid radical formation after multi-photon excitation of 8′-apo-β-carotenal†

Václav Šebelík, Valentyna Kuznetsova, Ivana Šímová and Tomáš Polívka *

Received 16th November 2024,
Accepted 16th February 2025

DOI: 10.1039/d4cp04373a

rsc.li/pccp

Carotenoids containing a conjugated C=O group exhibit complex excited-state dynamics that are influenced by solvent polarity due to the involvement of an intramolecular charge transfer (ICT) state. Our study explores the excited-state behavior of 8′-apo-β-carotenal under multi-photon excitation conditions. Using near-infrared (1300 nm) multi-photon excitation, we observe the formation of a cation radical of 8′-apo-β-carotenal, a process distinct from those following one-photon visible or UV excitation. Our findings suggest that this radical formation results from multi-photon excitation involving a higher-lying dark state, supported by intensity-dependent experiments. This work demonstrates that radical generation is a characteristic of this higher excited state and is not produced during relaxation from the S_1/ICT state. The results open new pathways for understanding carotenoid radical formation mechanisms under intense multi-photon excitation.

Introduction

Keto-carotenoids containing a conjugated C=O group have been extensively studied since the seminal study by Bautista *et al.*, who demonstrated that the excited-state dynamics of these carotenoids depend on solvent polarity.[1] This dependence was attributed to the presence of an intramolecular charge transfer (ICT) state that is coupled to the lowest carotenoid excited state, S_1, forming an S_1/ICT state, thereby modifying the lifetime of the lowest excited state.[1–5] The S_1/ICT lifetime shortening in polar solvents is always accompanied by new spectral bands in transient absorption spectra associated with the ICT state: the ICT excited state absorption band that is red shifted from the main $S_1 \rightarrow S_N$ transition[1,6] and ICT stimulated emission band in the near-IR spectral region.[2] Polarity-induced effects were also reported for the keto-carotenoid absorption band associated with the $S_0 \rightarrow S_2$ transition. While in non-polar solvents the characteristic three-peak absorption spectrum with well-resolved vibrational bands is observed, in polar solvents the resolution of the vibrational bands is significantly diminished, and the absorption band is broadened.[3,7–10]

While the first reports on polarity-induced effects in keto-carotenoids targeted the biologically relevant keto-carotenoids peridinin and fucoxanthin, which occur in photosynthetic antenna of dinoflagellates and diatoms,[11,12] another prototypical keto-carotenoid is 8′-apo-β-carotenal, which also exhibits a strong polarity-induced effect[13] and is readily available as it is used as a food colorant.[14–16] Excited state processes of 8′-apo-β-carotenal were first reported in 1986[17] and detailed exploration of the dependence of the excited state dynamics on solvent polarity was provided later:[13,18–20] the lifetime of the lowest excited state in nonpolar solvents is ~25 ps, and it is shortened to ~8 ps in polar solvents such as methanol or acetonitrile. In polar solvents, a pronounced ICT band appears around 650 nm, reaching about 70–80% of the intensity of the $S_1 \rightarrow S_N$ band peaking at ~560 nm.[13,20]

All information about excited-state properties of 8′-apo-β-carotenal is obtained from transient absorption experiments exciting the S_2 state because of the forbidden nature of the $S_0 \rightarrow S_1$ transition, preventing direct excitation of the S_1 (or ICT) state by one-photon transition. Thus, the S_1/ICT state, which is typically described as a double-well potential surface at which the S_1-like and ICT-like minima are separated by a polarity-dependent barrier,[5] is consistently formed through relaxation from the S_2 state. This complicates data interpretation as the S_1/ICT is populated with excess energy and the distribution of population between the S_1 and ICT minima may depend on the excitation wavelength.[21] Thus, it is of interest to design experiments in which the S_1/ICT could be excited directly.

Direct excitation of the S_1 state in the transient absorption experiment can be in principle achieved *via* two-photon excitation as demonstrated in a few experiments reported earlier.[22–26] These studies showed that excitation in the 1100–1300 nm spectral region generates typical transient absorption signals associated with the S_1 state, proving that the S_1 state is indeed possible to excite directly *via* two-photon excitation. These experiments also identified subtle differences between

Department of Physics, Faculty of Science, University of South Bohemia, Czech Republic. E-mail: tpolivka@prf.jcu.cz

† Electronic supplementary information (ESI) available. See DOI: https://doi.org/10.1039/d4cp04373a

one- and two-photon excited S_1 signals, such as generation of carotenoid triplets or radicals in some cases.[23–25] Detailed excitation intensity-dependent studies even demonstrated that multi-photon excitation is likely involved in the generation of signals after intense excitation in the near-IR spectral region.[23] A two-photon excited transient absorption experiment was also reported for the keto-carotenoid fucoxanthin,[27] showing that tuning the two-photon excitation wavelength has the ability to selectively excite either the S_1 or ICT part of the S_1/ICT potential surface.

Here, we report on the near-IR (1300 nm) excitation study of the keto-carotenoid 8′-apo-β-carotenal. Contrary to previous experiments, we have extended the probing window to the near-IR spectral region, which has allowed us to identify and monitor the formation of a cation radical of 8′-apo-β-carotenal. Detailed intensity dependence analysis demonstrated that the carotenoid radical is generated *via* multi-photon excitation of a previously unidentified dark excited state.

Materials and methods

Experimental details

A Spitfire Ace regenerative amplifier system (Spectra Physics), seeded with a Ti:sapphire oscillator (MaiTai SP, Spectra Physics) and pumped by an Nd:YLF laser (Empower 30, Spectra Physics), producing 4 mJ pulses centered at 800 nm with a 1 kHz repetition rate and a pulse duration of ∼100 fs, was used for generating excitation (pump) and probe pulses. The near-IR excitation beam was generated through parametric amplification (TOPAS Prime, Light Conversion). The pump beam was focused on the sample by a lens with a focal length of 500 mm. The pump intensity was set to 7×10^{16} photons per pulse cm^2, corresponding to 15 mW excitation power at 1300 nm. A fraction of the 800 nm beam from the Spitfire Ace was sent to the home-built non-collinear optical parametric amplifier in order to produce a 1250 nm beam used to generate the white-light supercontinuum (WLC) probe beam by focusing it to a 2 mm sapphire plate. The polarization between pump and probe beams was set parallel by a $\lambda/2$ waveplate. The signal-to-noise ratio was enhanced by splitting the WLC to reference and probe beams, both detected by a double CCD array in a prism spectrograph. This detection system allowed us to collect the data in a broad spectral range from 500 to 900 nm. The coherent artifact region (*ca.* −0.04 to 0.7 ps) was removed from the data. The same arrangement was used for the one-photon excitation (1PE) experiments with excitation wavelengths at 280 and 480 nm except that the 1PE intensity was set to $\sim 10^{14}$ photons per pulse cm^2. The obtained data sets were fitted using CarpetView software (Light Conversion, Lithuania) with a sequential model providing evolution-associated difference spectra (EADS).[28] The pump power dependence experiments were carried out to test nonlinearity of the obtained signals.

Sample preparation

8′-apo-β-carotenal was purchased from Sigma-Aldrich (≥96%, UV). The sample was stored in the dark at −40 °C prior to the experiment. For the transient absorption measurement, the sample was dissolved in *n*-hexane and methanol to yield OD ∼ 0.75 mm^{-1}. The experiment was carried out at room temperature with the sample mixed by a magnetic stirrer bar within a 2-mm quartz cuvette. Steady-state absorption spectra were measured before and after experiments to check for photodegradation of the sample. Some degradation was observed in the polar methanol (∼15%), a part of which could be due to *trans–cis* isomerization due to a slight increase of absorption in the 330–350 nm spectral region, while almost no degradation occurred when the carotenoid was dissolved in hexane (Fig. S1, ESI†).

Results

Ground state absorption

Fig. 1 shows the absorption spectra of 8′-apo-β-carotenal dissolved in two different solvents: non-polar *n*-hexane and polar methanol. Solvent polarity induces the effects described earlier.[13] In *n*-hexane, the spectrum is narrower and shows three well resolved 0-0, 0-1, and 0-2 vibronic bands related to the $S_0 \rightarrow S_2$ electronic transition. This contrasts with the spectrum in methanol, where these vibrational bands are much less defined, which is a common characteristic for carbonyl-containing carotenoids dissolved in polar solvents.[6,29] However, the solvent change does not notably alter the energy level of the S_2 state. No other absorption bands, such as a *cis* peak, are evident in the spectra. Even though 8′-apo-β-carotenal does not possess the ideal C_{2h} symmetry, there are no signs of the $S_0 \rightarrow S_1$ transition found in either of the steady-state absorption spectra.

Excited state absorption and dynamics

Previous research on carotenoids with similar conjugation lengths, which studied weak S_1 emission and $S_1 \rightarrow S_2$ transition energies, allows us to estimate the peak of the 0-0 band of the $S_0 \rightarrow S_1$ transition between 14 880 and 15 580 cm^{-1} (642 to 672 nm) for 8′-apo-β-carotenal.[7] This range is highlighted with a gray rectangle in Fig. 1. Given that the energy of the S_1 state of 8′-apo-β-carotenal can only be estimated we have selected the excitation wavelength 1300 nm to reach the two-photon energy close to the expected peak of the 0-0 band of the $S_0 \rightarrow S_1$ transition. This wavelength also falls into the spectral region where both solvents have minimal absorption (Fig. S2, ESI†).

Transient absorption spectra measured after excitation of 8′-apo-β-carotenal at 1300 nm in *n*-hexane and methanol are shown in Fig. 2. In *n*-hexane, the main peak is at ∼550 nm and is due to the $S_1 \rightarrow S_N$ transition as the spectral profile of this peak is comparable to that obtained in previous one-photon excitation studies of 8′-apo-β-carotenal in *n*-hexane,[13,20] proving that the 1300 nm excitation generates S_1 population. On the high energy side of the $S_1 \rightarrow S_N$ peak, there is a shoulder usually attributed to the S* state, observed previously in both one- and two-photon excitation experiments.[25,30–32] In the 600–700 nm region, two weak bands, which are associated with asymmetry of the conjugated system induced by the carbonyl group, are clearly visible even in the non-polar *n*-hexane.[13,20] In the near-IR spectral region, another

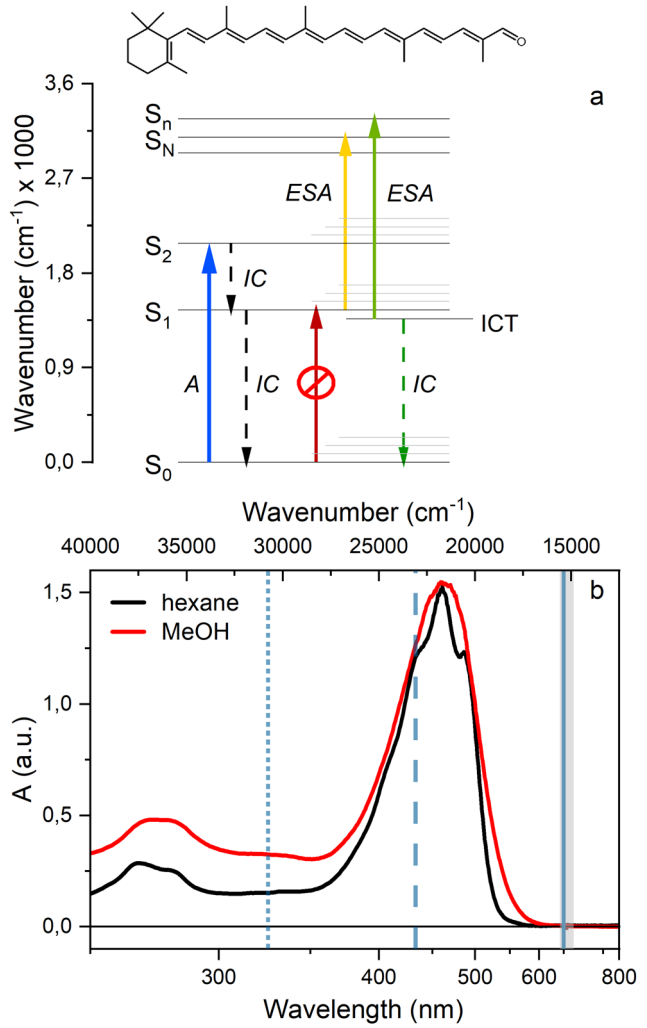

Fig. 1 (a) Energy level scheme of a carbonyl carotenoid with characteristic transitions, where A, ESA, and IC mean absorption, excited state absorption, and internal conversion, respectively; the structure of 8′-apo-β-carotenal is also shown. (b) Steady-state absorption spectrum of the 8′-apo-β-carotenal in methanol and *n*-hexane. The narrow gray rectangle marks the expected energy of the 0-0 band of the $S_0 \rightarrow S_1$ transition. The solid, dashed, and dotted vertical lines represent the two-, three-, and four-photon excitation energies, respectively.

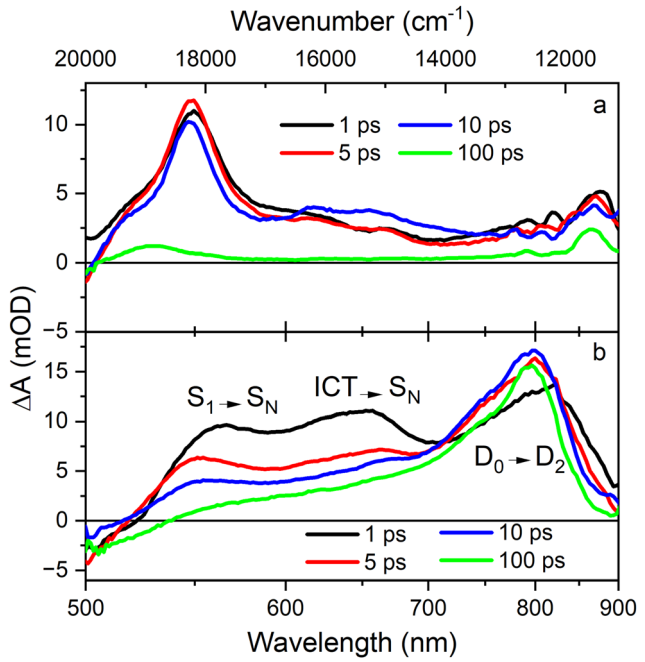

Fig. 2 Transient absorption spectra of 8′-apo-β-carotenal in (a) *n*-hexane and (b) methanol after 1300 nm multi-photon excitation with 15 mW pump power. To mitigate data noise, the *n*-hexane 100 ps curve was derived by averaging the values between 95 and 115 ps.

weak positive band is located at 880 nm. It has a lifetime longer than the $S_1 \rightarrow S_N$ band as it decays only slightly over the first 100 ps and likely corresponds to a cation radical of 8′-apo-β-carotenal. Moreover, the 100 ps transient spectrum also contains a weak positive feature peaking around 530 nm, which does not decay on the time scale of our experiment. Based on the spectral position and long lifetime of this band, we attribute this signal to a triplet state.

The transient absorption spectrum changes significantly when 8′-apo-β-carotenal is dissolved in methanol. The $S_1 \rightarrow S_N$ transition band is red shifted to 565 nm at 1 ps, but it is not the dominant peak anymore. The increased polarity enhances the bands in the 600–700 nm region, generating the characteristic broad ICT band, which is even stronger than the $S_1 \rightarrow S_N$ transition. This contrasts with earlier data obtained after direct excitation of the S_2 state,[13] but the enhanced amplitude of the ICT band observed here is due to overlap with the blue part of the strong spectral band peaking at 800 nm. Enhancement of this band in the polar solvent methanol supports the assignment of this feature to the 8′-apo-β-carotenal radical, because polar solvents stabilize the charge on the carotenoid cation radical. It is stabilized during the first 10 ps as it exhibits a blue shift from 820 to 800 nm between 1 and 10 ps. The carotenoid radical band almost does not decay within the time window of the experiment (Fig. 2).

Not only the spectral features but also the lifetimes of individual states of the carbonyl carotenoids are affected by the solvent polarity, as reported earlier also for the 8′-apo-β-carotenal.[13,20] The typical behavior of carbonyl carotenoids is a shortening of the S_1/ICT lifetime in polar solvents. This also applies for 8′-apo-β-carotenal excited at 1300 nm and the decays of the key spectral features are shown in Fig. 3. The prolongation of the S_1/ICT lifetime in *n*-hexane compared to methanol is obvious as well as the long lifetime of the cation radical in the near-IR spectral region. Interestingly, in methanol, the slow rise of the cation radical signal at 800 nm matches the decay of the transient $S_1 \rightarrow S_N$ band at 555 nm.

To obtain lifetimes of individual processes, the global fitting procedure using a sequential relaxation scheme was employed. The results of the analysis are shown in Fig. 4. Each dataset required four time components to accurately fit the spectral evolution, represented by the evolution-associated difference spectra (EADS). In all datasets, the first EADS is related to the S_1/ICT state, and as in the case of two-photon excitation, it should be excited directly without depopulation from higher

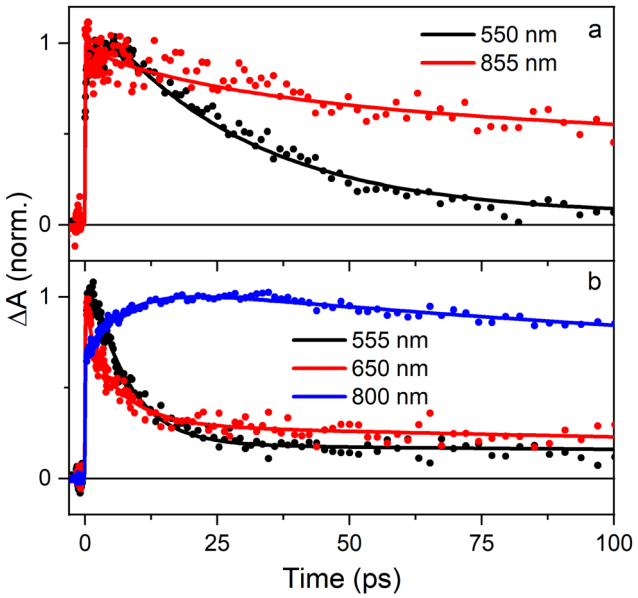

Fig. 3 Kinetics of 8′-apo-β-carotenal in (a) *n*-hexane and (b) methanol after 1300 nm multi-photon excitation with 15 mW pump power. The kinetics are shown at the wavelengths corresponding to the maxima of the $S_1 \rightarrow S_N$, ICT $\rightarrow S_N$, and $D_0 \rightarrow D_2$ transitions.

energy states. Also, due to significant interference from the coherent artifact within the first 0.5 ps, we cannot reliably assign sub-picosecond dynamics. In methanol, the S_1 band is accompanied by the ICT band typical for carbonyl carotenoids in polar solvents. As expected, the ICT amplitude is likely affected by the strong 800 nm cation radical band, which is also present in the first EADS spectrum, meaning that the radical must be generated within the first picosecond. Both S_1 and 800 nm bands exhibit signs of relaxation on the picosecond time scale. The relaxation process can be inferred from the peak narrowing and blue shift observed between the first and second EADS. The second EADS can be considered as depicting a relaxed S_1/ICT state with a polarity-dependent lifetime. In the non-polar *n*-hexane, the lifetime is 28 ps, and the polar methanol shortens the lifetime to 7 ps in agreement with earlier data obtained after one-photon excitation of the S_2 state.[13,18] It is important to note that the 7 ps process characterized by transition from the second (red) to third (blue) EADS also forms the final shape of the cation radical band. Since there is also an isosbestic point around 710 nm, clearly visible in both data (Fig. 2) and fits (Fig. 4), it may suggest that a part of the cation radical signal could be generated from the S_1/ICT state. Yet, since the signal from the carotenoid radical is clearly visible already in the first EADS, it is likely that similarity of the dynamics of the S_1/ICT decay and cation radical stabilization is rather coincidental. The third and fourth EADS are free of S_1 and ICT signatures and the only spectral features remaining are the 800 nm peak and the carotenoid triplet.

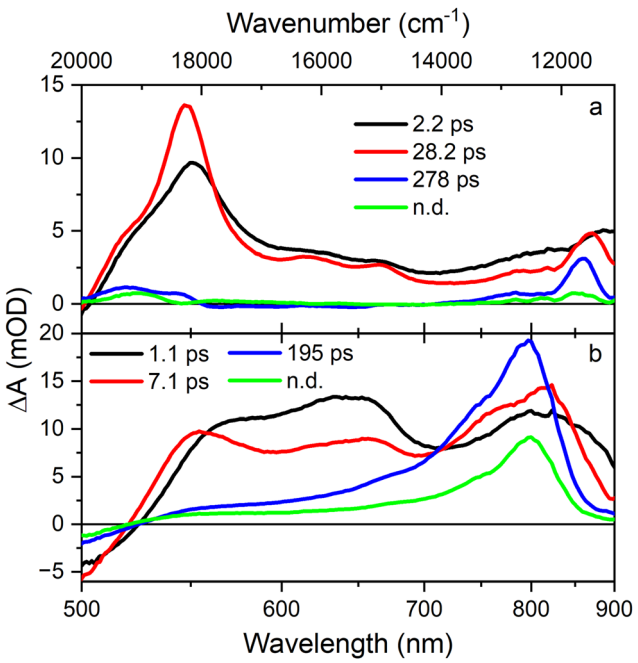

Fig. 4 EADS obtained from global fitting of multi-photon excitation transient absorption data of 8′-apo-β-carotenal in *n*-hexane (a), and methanol (b) after 1300 nm excitation. Both samples were excited by the 15 mW pump.

To justify the expected nonlinearity of the signal generated after excitation at 1300 nm, we have carried out excitation intensity dependence of the signal at the three key wavelengths corresponding to the maxima of the transient $S_1 \rightarrow S_N$ band in both solvents and the peak of the radical cation in methanol. The results are presented in Fig. 5. The data clearly indicate that the slope of the linear fit in the logarithmic plot is approximately four, and thus does not support the notion that the signal after 1300 nm excitation is due to two-photon excitation of the S_1/ICT state. Instead, the value rather points to a four-photon excitation of some higher-lying state, a picture comparable to that reported earlier for β-carotene.[23,33]

Discussion

The data presented in previous paragraphs demonstrate that in addition to the typical features observed in transient absorption spectra of 8′-apo-β-carotenal related to the S_1 and ICT bands, excitation at 1300 nm also produces a carotenoid radical and, solely in *n*-hexane, a weak signal from the carotenoid triplet. These new species, which are absent in experiments using excitation *via* the allowed $S_0 \rightarrow S_2$ transition, therefore must be related to the multi-photon nature of excitation as 8′-apo-β-carotenal has no linear absorption at 1300 nm. Surprisingly, the excitation intensity dependence shown in Fig. 5 indicates that the observed signal is not produced *via* two-photon excitation of the S_1/ICT state, but a dependence close to four-photon excitation occurs instead. It is important to stress that in our earlier experiments on lutein using the same experimental setup and excitation wavelengths, and comparable excitation intensities, we have observed intensity dependence identifying a clear two-photon excitation.[26] Thus, whether two- or multi-photon excitation dominates in a

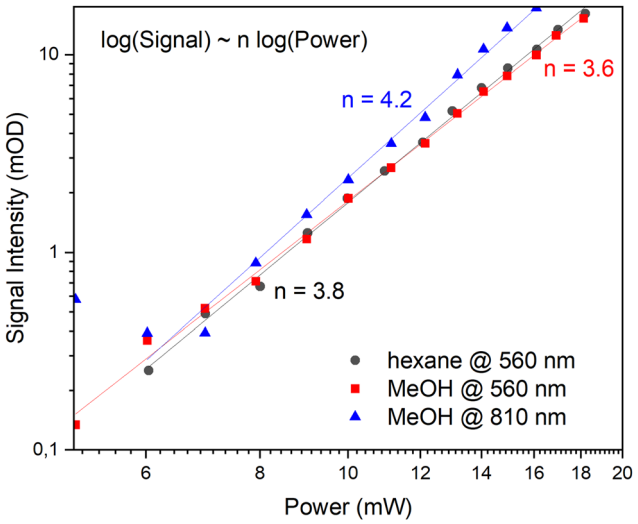

Fig. 5 Dependence of signal amplitude on pump intensity at several wavelengths after excitation at 1300 nm at 2 ps in *n*-hexane and methanol. The numbers indicate the slope of the respective fitting curves.

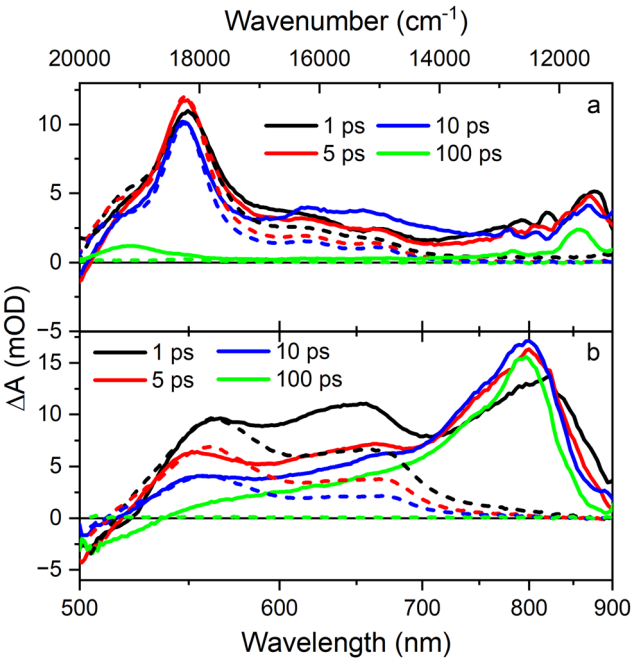

Fig. 6 Comparison of transient absorption spectra of 8′-apo-β-carotenal in (a) *n*-hexane and (b) methanol after 1300 nm multi-photon excitation (solid lines) and UV excitation at 280 nm (dashed lines). To mitigate noise, the 100 ps curve obtained after multi-photon excitation of 8′-apo-β-carotenal in *n*-hexane is shown as the average of all spectra measured between 95 and 115 ps.

particular experiment is likely dependent on the carotenoid structure.

The observation that the signal measured here is a result of a four-photon excitation changes our assumption that we directly excite the S_1/ICT state. Instead, some higher-lying excited state located around 325 nm (~30 770 cm^{-1}), thus far higher than the S_2 state, is primarily excited. Clearly, this excited state is forbidden for one photon transition from the ground state as evidenced by minimal ground state absorption in this spectral region (Fig. 1). The observation of the strong signal from a carotenoid radical already at 1 ps after 1300 nm excitation (Fig. 2) provides further evidence that the state primarily excited in this experiment is not the S_1/ICT, because this state, if populated *via* relaxation from the S_2 state, does not produce a carotenoid radical as reported in a number of previous experiments.[29,34]

Since our data points to the conclusion that the carotenoid radical is formed from a dark excited state located above the S_2 state, the radical could be also generated if a higher-lying excited state is excited directly *via* one-photon excitation in the UV spectral region. This is indeed possible as essentially all carotenoids have a UV absorption band located in the 250–300 nm spectral region corresponding to a transition to the S_{UV} state.[34] For 8′-apo-β-carotenal the S_{UV} band has the lowest vibrational peak at ~280 nm in both methanol and *n*-hexane (Fig. 1). Thus, to test this hypothesis, we have excited the S_{UV} band at 280 nm and transient absorption spectra obtained in this experiment are in Fig. 6 compared to those measured after multi-photon excitation. No carotenoid radical is produced by the 280 nm excitation, and transient spectra are nearly identical to those measured when the S_2 state is excited at 480 nm (Fig. S3, ESI†). The excited-state dynamics after 280 nm excitation are similar to those obtained earlier after 480 nm excitation as evidenced by global fitting analysis of the UV excited data (Fig. S4, ESI†). Absence of any signal from the carotenoid radical after 1PE of either the S_{UV} or S_2 state further supports the hypothesis that carotenoid radicals cannot be generated from the S_1/ICT state, even though the time scales related to decay if the S_1/ICT state and stabilization of the carotenoid radical are similar.

While this agrees with previous experiments using UV excitation of carotenoids in which a carotenoid radical has never been reported,[34–36] it is rather surprising in the context of the experiment reported here. Obviously, the state excited at 280 nm should have enough energy to generate radicals as it must be higher than the dark state excited *via* the four-photon excitation at 1300 nm (~325 nm). However, the radical is not produced, meaning that there is no pathway to radical formation from the S_{UV} state, and relaxation of the S_{UV} state excited at 280 nm bypasses the radical precursor, which can be achieved only *via* multi-photon excitation.

A hypothesis offered by Buckup *et al.*[23] suggested that multi-photon excitation may directly excite a doublet state, which would explain why the radical is not observed after one-photon excitation of the S_{UV} state. It is also worth noting that carotenoid radicals were reported after the 'ladder' excitation of astaxanthin in a pump–repump experiment called resonant-2-photon-2-color-ionization (R2P2CI).[37,38] In this experiment, the first excitation pulse at around 500 nm excites the S_2 state, while the second pulse arriving within the 100 fs is at around 1000 nm and thus resonant with the $S_2 \rightarrow S_N$. In such arrangement, which excites an upper excited state located around 30 000 cm^{-1}, radicals of a few different carotenoids

have been reported.[37–39] As well as in our experiment described here, these experiments provide evidence that carotenoid radicals can be generated from a state having energy of $\sim$30 000 cm^{-1}, thus below the S_{UV} state which, when excited directly *via* one-photon excitation in UV, does not produce carotenoid radicals (Fig. 6).[34,36] Interestingly, no carotenoid radical was reported in a pump–repump experiment in which the $S_1 \rightarrow S_N$ transition was re-excited.[36]

Thus, a comparison of our data with earlier experiments suggests that the production of a carotenoid radical relates to multi-photon or 'ladder' excitation of an excited state located around 30 000 cm^{-1}, while one-photon excitation, even with higher photon energies, cannot produce the radical. This could be due to a configuration of the relaxed ground state, which could be unfavorable to produce radicals. Upon ladder excitation, however, the configuration of the intermediate state may enable a pathway that leads to the formation of the carotenoid radical. If this hypothesis is valid though, it would mean that in our multi-photon excitation experiment, we must be in the condition of a 'pseudo-ladder' excitation involving population of some intermediate state. Since our data does not allow for analyzing the very early delay times after excitation due to strong coherent artifacts in the first 500 fs, we cannot verify this hypothesis. The verification awaits for future multi-photon experiments, which should target the early dynamics after excitation.

Conclusions

Based on analysis of broadband transient absorption data obtained for 8′-apo-β-carotenal after NIR excitation at 1300 nm we conclude that, in contrast to the original assumption that NIR excitation induces a two-photon excitation of the S_1/ICT state, such excitation conditions lead predominantly to a multi-photon excitation of a dark excited state located above the strongly absorbing S_2 state. This state is a precursor of a carotenoid radical, though in the nonpolar *n*-hexane, in which the radical is not stabilized, it also opens a pathway to the triplet state. The radical precursor state must have a specific configuration as it cannot be excited by one-photon excitation from the ground state, even if UV excitation with energy above the radical precursor state is used. Our results show that in any multi-photon excitation experiments on carotenoids, intensity-dependent data are critical for data analysis and interpretation. Whether the obtained data results from two-photon[22,26,40] or multi-photon[23] excitation can be decided only from analysis of the intensity-dependent data. Clearly, carotenoid structure as well as the used solvent can be decisive factors as to whether two- or multi-photon excitation dominates.

Data availability

The key data are presented directly in the article. Raw, unprocessed spectroscopic datasets are available directly from the authors upon request.

Conflicts of interest

There are no conflicts to declare.

Acknowledgements

Financial support was provided by the Czech Science Foundation grant 19-28323X.

Notes and references

1 J. A. Bautista, R. E. Connors, B. B. Raju, R. G. Hiller, F. P. Sharples, D. Gosztola, M. R. Wasielewski and H. A. Frank, *J. Phys. Chem. B*, 1999, **103**, 8751–8758.
2 D. Zigmantas, T. Polívka, R. G. Hiller, A. Yartsev and V. Sundström, *J. Phys. Chem. A*, 2001, **105**, 10296–10306.
3 D. Zigmantas, R. G. Hiller, A. Yartsev, V. Sundström and T. Polívka, *J. Phys. Chem. B*, 2003, **107**, 5339–5348.
4 K. Redeckas, V. Voiciuk and M. Vengris, *Photosynth. Res.*, 2016, **128**, 169–181.
5 R. G. West, M. Fuciman, H. Staleva-Musto, V. Šebelík, D. Bína, M. Durchan, V. Kuznetsova and T. Polívka, *J. Phys. Chem. B*, 2018, **122**, 7264–7276.
6 H. A. Frank, J. A. Bautista, J. Josue, Z. Pendon, R. G. Hiller, F. P. Sharples, D. Gosztola and M. R. Wasielewski, *J. Phys. Chem. B*, 2000, **104**, 4569–4577.
7 T. Polívka and V. Sundström, *Chem. Rev.*, 2004, **104**, 2021–2071.
8 P. O. Andersson, T. Gillbro, L. Ferguson and R. J. Cogdell, *Photochem. Photobiol.*, 1991, **54**, 353–360.
9 H. Nagae, M. Kuki, R. J. Cogdell and Y. Koyama, *J. Chem. Phys.*, 1994, **101**, 6750–6765.
10 M. Kuki, H. Nagae, R. J. Cogdell, K. Shimada and Y. Koyama, *Photochem. Photobiol.*, 1994, **59**, 116–124.
11 K. Seth, A. Kumar, R. P. Rastogi, M. Meena, V. Vinayak and H. Harish, *Algal Res.*, 2021, **60**, 102475.
12 Y. Bai, T. Cao, O. Dautermann, P. Buschbeck, M. B. Cantrell, Y. Chen, C. D. Lein, X. Shi, M. A. Ware, F. Yang, H. Zhang, L. Zhang, G. Peers, X. Li and M. Lohr, *Proc. Natl. Acad. Sci. U. S. A.*, 2022, **119**, e2203708119.
13 M. Durchan, M. Fuciman, V. Šlouf, G. Keşan and T. Polívka, *J. Phys. Chem. A*, 2012, **116**, 12330–12338.
14 A. Mortensen, *Pure Appl. Chem.*, 2006, **78**, 1477–1491.
15 W. Jang, C. Lee, H. J. Suh and J. Lee, *Food Sci. Biotechnol.*, 2023, **32**, 1501–1513.
16 M. Rodriguez-Concepcion, J. Avalos, M. L. Bonet, A. Boronat, L. Gomez-Gomez, D. Hornero-Mendez, M. C. Limon, A. J. Meléndez-Martínez, B. Olmedilla-Alonso, A. Palou, J. Ribot, M. J. Rodrigo, L. Zacarias and C. Zhu, *Prog. Lipid Res.*, 2018, **70**, 62–93.
17 M. R. Wasielewski and L. D. Kispert, *Chem. Phys. Lett.*, 1986, **128**, 238–243.
18 F. Ehlers, D. A. Wild, T. Lenzer and K. Oum, *J. Phys. Chem. A*, 2007, **111**, 2257–2265.
19 M. Kopczynski, F. Ehlers, T. Lenzer and K. Oum, *J. Phys. Chem. A*, 2007, **111**, 5370–5381.

20 K. Horiuchi, C. Uragami, R. Tao, D. Kosumi, R. J. Cogdell and H. Hashimoto, *Molecules*, 2023, **28**, 4424.
21 D. Kosumi, T. Kusumoto, R. Fujii, M. Sugisaki, Y. Iinuma, N. Oka, Y. Takaesu, T. Taira, M. Iha, H. A. Frank and H. Hashimoto, *Phys. Chem. Chem. Phys.*, 2011, **13**, 10762–10770.
22 P. J. Walla, P. A. Linden, C. P. Hsu, G. D. Scholes and G. R. Fleming, *Proc. Natl. Acad. Sci. U. S. A.*, 2000, **97**, 10808–10813.
23 T. Buckup, A. Weigel, J. Hauer and M. Motzkus, *Chem. Phys.*, 2010, **373**, 38–44.
24 D. Kosumi, K. Abe, H. Karasawa, M. Fujiwara, R. J. Cogdell, H. Hashimoto and M. Yoshizawa, *Chem. Phys.*, 2010, **373**, 33–37.
25 V. Šebelík, M. Fuciman, R. G. West and T. Polívka, *Chem. Phys.*, 2019, **522**, 171–177.
26 V. Šebelík, V. Kuznetsova, H. Lokstein and T. Polívka, *J. Phys. Chem. Lett.*, 2021, **12**, 3176–3181.
27 D. Kosumi, T. Kusumoto, R. Fujii, M. Sugisaki, Y. Iinuma, N. Oka, Y. Takaesu, T. Taira, M. Iha, H. A. Frank and H. Hashimoto, *Chem. Phys. Lett.*, 2009, **483**, 95–100.
28 I. H. M. Van Stokkum, D. S. Larsen and R. Van Grondelle, *Biochim. Biophys. Acta, Bioenerg.*, 2004, **1657**, 82–104.
29 D. Zigmantas, R. G. Hiller, F. P. Sharples, H. A. Frank, V. Sundström and T. Polívka, *Phys. Chem. Chem. Phys.*, 2004, **6**, 3009–3016.
30 C. C. Gradinaru, J. T. M. Kennis, E. Papagiannakis, I. H. M. Van Stokkum, R. J. Cogdell, G. R. Fleming, R. A. Niederman and R. Van Grondelle, *Proc. Natl. Acad. Sci. U. S. A.*, 2001, **98**, 2364–2369.
31 V. Balevičius, D. Abramavicius, T. Polívka, A. Galestian Pour and J. Hauer, *J. Phys. Chem. Lett.*, 2016, **7**, 3347–3352.
32 T. Lenzer, F. Ehlers, M. Scholz, R. Oswald and K. Oum, *Phys. Chem. Chem. Phys.*, 2010, **12**, 8832–8839.
33 D. Kosumi, M. Fujiwara, H. Hashimoto and M. Yoshizawa, *J. Phys. Soc. Jpn.*, 2009, **78**, 104715.
34 T. Khan, R. Litvín, V. Šebelík and T. Polívka, *ChemPhysChem*, 2021, **22**, 471–480.
35 H. H. Billsten, J. Pan, S. Sinha, T. Pascher, V. Sundström and T. Polívka, *J. Phys. Chem. A*, 2005, **109**, 6852–6859.
36 V. Kuznetsova, M. Fuciman and T. Polívka, *Phys. Chem. Chem. Phys.*, 2023, **25**, 22336–22344.
37 S. Amarie, J. Standfuss, T. Barros, W. Kühlbrandt, A. Dreuw and J. Wachtveitl, *J. Phys. Chem. B*, 2007, **111**, 3481–3487.
38 S. Amarie, U. Förster, N. Gildenhoff, A. Dreuw and J. Wachtveitl, *Chem. Phys.*, 2010, **373**, 8–14.
39 E. Papagiannakis, M. Vengris, D. S. Larsen, I. H. M. Van Stokkum, R. G. Hiller and R. Van Grondelle, *J. Phys. Chem. B*, 2006, **110**, 512–521.
40 D. A. Gacek, A. Betke, J. Nowak, H. Lokstein and P. J. Walla, *Phys. Chem. Chem. Phys.*, 2021, **23**, 8731–8738.

